Transp Porous Med (2012) 95:285–303
DOI 10.1007/s11242-012-0043-8

Dependency of Tortuosity and Permeability of Porous Media on Directional Distribution of Pore Voids

Peijun Guo

Received: 25 April 2012 / Accepted: 3 July 2012 / Published online: 25 July 2012

Abstract Single-phase fluid flow in porous media is usually direction dependent owing to the tortuosity associated with the internal structures of materials that exhibit inherent anisotropy. This article presents an approach to determine the tortuosity and permeability of porous materials using a structural measure quantifying the anisotropic distribution of pore voids. The approach uses a volume averaging method through which the macroscopic tortuosity tensor is related to both the average porosity and the directional distribution of pore spaces. The permeability tensor is derived from the macroscopic momentum balance equation of fluid in a porous medium and expressed as a function of the tortuosity tensor and the internal structure of the material. The analytical results generally agree with experimental data in the literature.

Keywords Porous media · Anisotropy · Permeability · Tortuosity · Directional pore space distribution

1 Introduction

Since the pioneering study of Kozeny (1927), numerous studies have been performed to correlate the permeability of porous media with their physical properties, including porosity, pore size and structures, mean particle size and particle size distributions. In the various models in the literature, tortuosity is an important quantity that is used to bridge the pore structure and the macroscopic permeability (Dullien 1975; Bear and Bachmat 1990). The tortuosity is used to describe the difference between the actual distance traveled by fluid particles and the macroscopic travel distance, owing to the sinuosity and interconnectivity of pore spaces. Despite the extensive use of the concept of tortuosity, its definition is not unique. Geometric tortuosity is defined as the ratio between the shortest path of interconnected points in pore fluid space to the straight distance between these points. The hydraulic

P. Guo (✉)
Department of Civil Engineering, McMaster University, Hamilton, ON, L8S 4L7, Canada
e-mail: guop@mcmaster.ca

tortuosity factor appearing in the Kozeny–Carman equation (Carman 1937) is the ratio of the effective hydraulic path length (L_e) to the straight line distance (L) in the direction of flow and it can be very different from the geometric tortuosity (Clennell 1997). In general, tortuosity depends on various factors, including the shape, size, and type of the grains, pores, and pore channels; mode of packing of the grains; grain size distribution; the orientation and non-uniformity of the grains (Dullien 1979; Salem and Chilingarian 2000). However, the tortuosity factor is often expressed as a function of porosity ϕ in many different forms, e.g. $\tau(\phi) = \phi^{-p}$ (Bear 1972; Dullien 1979; Mota et al. 2001; Dias et al. 2006), $\tau(\phi) = 1 - p \ln \phi$ (Comiti and Renaud 1989; Mauret and Renaud 1997), $\tau(\phi) = 1 + p(1-\phi)$ (Weissberg 1963; Iversen and Jorgensen 1993; Boudreau and Meysman 2006), $\tau(\phi) = 1 + p\sqrt{1-\phi}$ (Duda et al. 2011). In these expressions, p is a certain constant. Even though the hydraulic tortuosity is directional dependent and should be described as a second-rank tensor (Bear and Bachmat 1990; Diedericks and Du Plessis 1995), the scalar tortuosity factor τ is generally used in the literature, even in some recent studies (Dias et al. 2006; Selomulya et al. 2006; Matyka et al. 2008; Gommes et al. 2009; Koza et al. 2009; Lanfrey et al. 2010; Yazdchi et al. 2011).

Different methods, either direct or indirect, have been developed to determine the tortuosity factor of porous materials, such as electrical resistance measurements (Mast and Potter 1963; Barrande et al. 2007), gas tracer tests (Kreamer et al. 1988) and hydraulic conductivity measurements (Witt and Brauns 1983; Comiti and Renaud 1989; Salem and Chilingarian 2000). More recently, advanced digital image analysis techniques including X-ray microtomography are used for 3D imaging of solid (or void) structures, from which the tortuosity can be estimated based on geodesic reconstruction. When the reconstructed void structures are available, flow in the porous media can be simulated using the Lattice-Boltzmann method (LBM) and the permeability can be determined correspondingly (Al-Omari and Masad 2004; Selomulya et al. 2006; Gommes et al. 2009; Gao et al. 2012; Khan et al. 2012).

Even though most experimental studies expressed the tortuosity as a scalar function of porosity, evidence of directional variation of tortuosity is not scarce in the literature, either based on the anisotropic permeability (Scheidegger 1954; Rice et al. 1970; Dullien 1975; Witt and Brauns 1983; Chapuis and Gill 1989; Salem and Chilingarian 2000), anisotropic diffusion processes (Greenkorn and Kessler 1970; Kim et al. 1987; Whitaker 1999; Ohkubo 2008) or geodesic reconstruction of pore space based on advanced digital image analysis (Selomulya et al. 2006). Theoretical analyses on the directional variation of tortuosity for discrete materials composed of mono-sized particles of similar shape and specific spatial distributions were reported (Daigle and Dugan 2011). In general, the hydraulic conductivity when flow is parallel to the bedding plane (i.e. perpendicular to the direction of sedimentation) is higher than that when flow is perpendicular to the bedding plane, which implies smaller tortuosity in directions parallel to the bedding plane (Witt and Brauns 1983; Chapuis and Gill 1989). Salem and Chilingarian (2000) investigated the tortuosity associated with different directions of flow in various porous media. They observed that the dependence of the tortuosity factor on porosity is governed greatly by the direction of flow because of the orientation, mineralogy and mode of packing of the grains as well as non-uniformity in the size and shape of the grains and pores. Daigle and Dugan (2011) theoretically examined the tortuosity anisotropy of porous media composed of flat cylindrical grains oriented at some angle with respect to the horizontal. For such periodic arrangements of particles of the same size, both the tortuosity and the permeability in the direction parallel to the bedding plane (horizontal) are higher than those perpendicular to the bedding plane, with the differences increasing as the porosity is increased. In addition, the ratio between the tortuosity factors in two arbitrary orthogonal directions varies with the bedding plane orientation. The theoretical results were

verified with simulations performed using the LBM, with the tortuosity determined from the hydraulic conductivity using the Kozeny–Carman equation.

Special attention should be paid to the comprehensive study relevant to tortuosity by Whitaker and co-workers (Whitaker 1986, 1999; Kim et al. 1987). Based on the method of volume averaging, for a representative region of a spatially periodic porous medium, the effective diffusivity tensor $\mathbf{D}'_{\text{eff}}$ is derived as a function of the unit normal vectors on the interfacial area within the averaging volume and a closure variable that is uniquely determined by the boundary conditions. By defining the tortuosity as the ratio between the molecular diffusion coefficient of the fluid and the effective diffusivity, it is identified that the tortuosity varies with the porosity, the particle geometry and the direction along which diffusion takes place. In other words, the effective diffusivity (and hence the tortuosity) parallel to the bedding plane is different from that normal to the bedding plane. The theoretical results are generally in agreement with experimental data.

However, when predicting the permeability of a porous medium, the tortuosity is required only by models based on pore structures. Tortuosity enters these models through the analysis for fluid flow in void space. Alternative approaches are available to estimate the anisotropy of permeability. For example, in the stochastic approach developed by Dagan (1989), the hydraulic conductivity K is described as a stationary space random function characterized by a lognormal distribution. The covariance of $Y = \ln K$ is represented by different correlation scales I_{h} and I_{v} in the horizontal plane and vertical direction, respectively, with the ratio $f = I_{\text{v}}/I_{\text{h}}$ being coined as the anisotropic ratio. The conductivity is then characterized entirely by the four parameters: K_{G} (the geometric mean of K), σ_Y^2 (the variance of Y), I_{h} and f. Dagan's original model was extended to determine the anisotropic conductivity of heterogeneous porous formations made up from inclusions (spheroids) of conductivity K_1 submerged in a matrix of conductivity K_0 (Jankovich et al. 2003; Suribhatla et al. 2011). The conductivity of the matrix can be either isotropic or anisotropic. It has been shown that the conductivity of the anisotropic formation is function of K_{G}, $K_{0\text{h}}/K_{\text{G}}$, $K_{0\text{v}}/K_{\text{G}}$, σ_Y^2, I_{h} and f. For inclusions of a periodic packing of particles, I_{h} can be related to the size of particles.

The study presented in this article investigates a different method to describe the anisotropy of tortuosity and permeability of saturated granular media using a volume averaging approach, by incorporating a continuum measure of internal structural disorder identified with the directional distribution of pore space in the material. In Sect. 2, a brief review is presented, focusing on the macroscopic description of flow in porous media based on the volume averaging. In Sect. 3, a probability density function that describes the spatial distribution of pore space is used as a measure for the anisotropic structure. Then the tortuosity tensor as defined by Bear and Bachmat (1990) is derived and expressed as a function of the spatial distribution of pore space in addition to the average porosity. Based on the macroscopic fluid momentum balance equation, the permeability is next related to the tortuosity tensor and eventually expressed as a function of both the average value of porosity and its spatial distribution. Finally, the results from the theoretical analysis are compared with experimental observations in the literature.

2 Macroscopic Description of Single-Phase Flow in Porous Media Based on Volume Averaging

2.1 Preliminary

The flow of water in a saturated granular material is described using an approach of local volume averaging taking into account mass balance on both the macro- and microlevels. For a

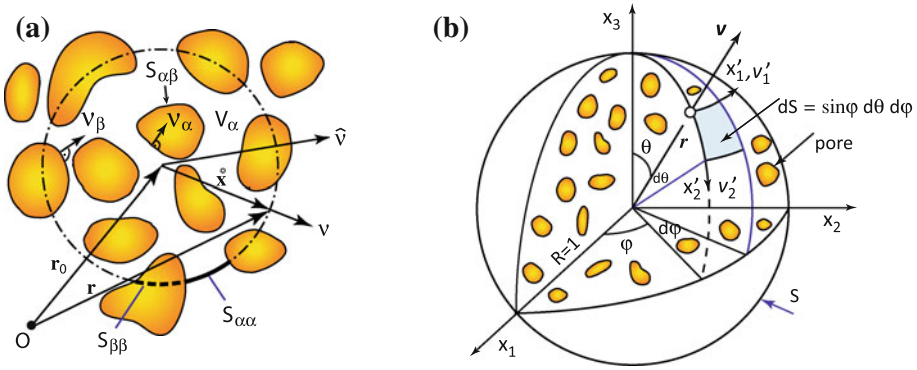

Fig. 1 **a** REV of a porous medium and **b** a unit sphere

unit sphere enclosing a representative element volume (REV) of the material consisting of α-(fluid) and β-(solid) phases as shown in Fig. 1a, let S_0 be the surface area of the sphere (with the radius of $R = 1$) encompassing the REV, $S_{\alpha\alpha}$ the area around the REV that intersects the fluid, $S_{\beta\beta}$ the area around the REV that crosses the particles and $S_{\alpha\beta}$ the total area of the interfaces between particles and the fluid. The total areas enclosing the unit sphere and the fluid are then $S_0 = S_{\alpha\alpha} + S_{\beta\beta}$ and $S_{0\alpha} = S_{\alpha\alpha} + S_{\alpha\beta}$, respectively. Following Bear and Bachmat (1990) and Whitaker (1999), the following averages of a function $e_\alpha(\mathbf{x})$ are defined:

Volumetric intrinsic phase average	$\bar{e}_\alpha^\alpha = \frac{1}{V_\alpha}\int_{V_\alpha} \bar{e}_\alpha \mathrm{d}V$
Volumetric phase average	$\bar{e}_\alpha = \frac{1}{V_0}\int_{V_\alpha} \bar{e}_\alpha \mathrm{d}V$
Areal intrinsic phase average	$\tilde{e}_{A\alpha}^\alpha = \frac{1}{S_{0\alpha}}\int_{A_\alpha} \bar{e}_\alpha \mathrm{d}S$
Areal average	$\tilde{e}_{A\alpha} = \frac{1}{S_0}\int_{A_\alpha} \bar{e}_\alpha \mathrm{d}S$

where $\mathrm{d}S = R^2 \sin\theta \mathrm{d}\theta\mathrm{d}\varphi$, $\mathrm{d}V = R^2 \sin\theta \mathrm{d}r\mathrm{d}\theta\mathrm{d}\varphi$, V_α and V_β are the volumes occupied by phases α and β respectively, while the total volume of the REV is $V_0 = V_\alpha + V_\beta$.

It should be emphasized that, in these definitions, V_α should be interpreted as the effective pore volume (Bear 1972) through which the fluid flows. Any non-interconnected pores, dead-end pores and stagnant pockets are referred to as ineffective pores, as shown in Fig. 2.

2.2 Flow in a REV of Porous Media

Following Bear and Bachmat (1990), the macroscopic momentum balance equation of the fluid in a porous medium is expressed as

$$\bar{\mu}_\alpha^\alpha \alpha_{ij} C_\alpha \phi_0 \frac{\bar{V}_{\alpha j}^\alpha - \bar{V}_{\beta j}^\beta}{\Delta_\alpha^2} = -\phi_0 T_{\alpha ij}^* \left(\frac{\partial \bar{p}^\alpha}{\partial x_j} + \bar{\rho}^\alpha g \frac{\partial z}{\partial x_j} \right), \tag{1}$$

where ϕ_0 is the porosity of the material defined as $\phi_0 = \phi_\alpha = V_\alpha / V_0$ for saturated porous media, μ_α is the dynamic viscosity of the fluid, C_α a shape factor related to pore sizes, while V_i, ρ and p are the velocity, density and pressure, respectively, the hydraulic radius Δ_α is

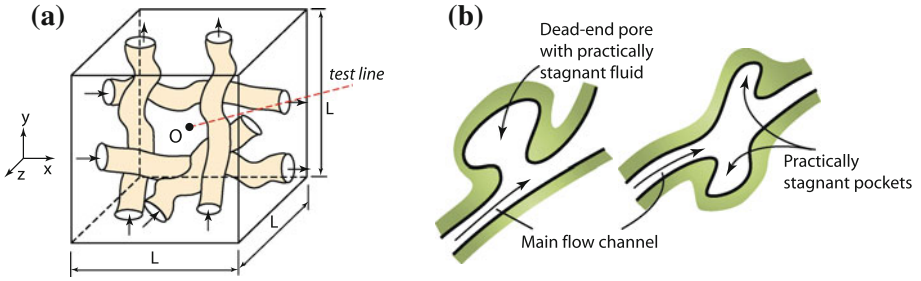

Fig. 2 **a** The REV of a isotropic porous system considered by Bachmat and Bear (1986); Bear and Bachmat (1990); **b** dead-end pores and stagnant pockets

the ratio of fluid volume to the fluid–solid interface area (i.e. $\Delta_\alpha = V_\alpha / S_{\alpha\beta}$), α_{ij} is defined as

$$\alpha_{ij} = \delta_{ij} - \widetilde{\nu_i \nu_j}^{\alpha\beta} = \delta_{ij} - \frac{1}{S_{\alpha\beta}} \int\limits_{S_{\alpha\beta}} \nu_{\alpha i} \nu_{\alpha j} \mathrm{d}S, \tag{2}$$

where δ_{ij} is the Kronecker delta function, $\nu_{\alpha i}$ the unit normal vector of $S_{\alpha\beta}$ (as shown in Fig. 1a). $T^*_{\alpha ij}$ is the tortuosity tensor defined as

$$T^*_{\alpha ij} = \frac{1}{V_\alpha} \int\limits_{S_{\alpha\alpha}} \overset{\circ}{x}_i \, \nu_{\alpha j} \mathrm{d}S \tag{3}$$

with $\overset{\circ}{\mathbf{x}} = \mathbf{r} - \mathbf{r}_0$, in which $\mathbf{r}$ and $\mathbf{r}_0$ are the position vectors of a point on $S_{\alpha\alpha}$ and the centre of the REV, respectively (see Fig. 1a). $\mathbf{T}^*_\alpha$ expresses the total static moment of the oriented areal element comprising the $S_{\alpha\alpha}$-surface, with respect to planes passing through the centroid of the REV, per unit volume of the α-phase within V_0. Bear and Bachmat (1990) gave the following expression for $\mathbf{T}^*_\alpha$:

$$T^*_{\alpha ij} = \frac{1}{V_\alpha} \int\limits_{S_{\alpha\alpha}} R \nu_{\alpha i} \nu_{\alpha j} \mathrm{d}S = \frac{\phi^S_\alpha S_0 R}{\phi_\alpha V_0} \frac{1}{S_{\alpha\alpha}} \int\limits_{S_{\alpha\alpha}} \nu_{\alpha i} \nu_{\alpha j} \mathrm{d}S = \frac{3\phi^S_\alpha}{\phi_\alpha} \widetilde{\nu_{\alpha i} \nu_{\alpha j}}^{\alpha\alpha} \tag{4}$$

In this expression, the term $\widetilde{\nu_{\alpha i} \nu_{\alpha j}}^{\alpha\alpha}$ represents the average of $\nu_{\alpha i} \nu_{\alpha j}$ on the $S_{\alpha\alpha}$-surface and reflects the effect of anisotropy on tortuosity, $\phi^S_\alpha = S_{\alpha\alpha}/S_0$ denotes the fraction of the $\alpha - \alpha$-surface in S_0 (i.e. the areal porosity in S_0), $\phi^S_\alpha / \phi_\alpha$ is considered as a measure of the tortuosity of the void space with $3\phi^S_\alpha / \phi_\alpha \leq 1$ (Bachmat and Bear 1986; Bear and Bachmat 1990). In general, the tortuosity tensor defined in Eq. (3) is a symmetric second-rank tensor.

For isotropic porous media, Bear and Bachmat (1990) assumed $\widetilde{\nu_{\alpha i} \nu_{\alpha j}}^{\alpha\alpha} = (1/3)\delta_{ij}$, which results in

$$T^*_{\alpha ij} = T^*_{\alpha 0} \delta_{ij}, \quad T^*_{\alpha 0} = \phi^S_\alpha / \phi_\alpha \tag{5}$$

The permeability tensor can be obtained from Eq. (1) as

$$k_{ij} = \frac{\phi_\alpha \Delta^2_\alpha}{C_\alpha} (\alpha_{il})^{-1} T^*_{\alpha lj} = \frac{\phi^3_\alpha}{C_\alpha \Sigma^2_{\alpha\beta}} (\alpha_{il})^{-1} T^*_{\alpha lj}. \tag{6}$$

By defining the specific area $\Sigma_{\alpha\beta} = S_{\alpha\beta}/V_0 = \phi_\alpha/\Delta_\alpha$ based on the bulk volume of the REV and $\Sigma^{\beta}_{\alpha\beta} = S_{\alpha\beta}/V_\beta = \phi_\alpha/[\Delta_\alpha(1-\phi_\alpha)] = \Sigma_{\alpha\beta}/(1-\phi_\alpha)$ based on the volume of solid particles, Eq. (6) becomes

$$k_{ij} = \frac{\phi_\alpha^3}{C_\alpha(1-\phi_\alpha)^2(\Sigma^{\beta}_{\alpha\beta})^2}\,(\alpha_{il})^{-1}\,T^*_{\alpha lj}. \tag{7}$$

For an isotropic medium, Bear and Bachmat (1990) further assumed $\alpha_{ij} = a\delta_{ij}$ with $a = 2/3$ and the permeability was derived as:

$$k = \frac{\phi_\alpha^3}{aC_\alpha(1-\phi_\alpha)^2(\Sigma^{\beta}_{\alpha\beta})^2} = \frac{\phi_\alpha\Delta_\alpha^2}{aC_\alpha}T^*_{\alpha 0}. \tag{8}$$

Recall the general expression of the Kozeny–Carman equation of permeability for one-dimensional flow (Carman 1937; Dullien 1979)

$$k_{\mathrm{KC}} = \frac{\phi_\alpha\Delta_\alpha^2}{C_0\tau^2};\quad \Delta_\alpha = \frac{\phi_\alpha}{(1-\phi_\alpha)\Sigma^{\beta}_{\alpha\beta}} \tag{9}$$

in which Δ_α is the hydraulic radius, τ is the tortuosity factor defined as the ratio of the 'effective average path length' L_e to the shortest distance measured along the direction of macroscopic flow L, i.e. $\tau = L_\mathrm{e}/L$. C_0 is a shape factor depending on the cross-sectional area of the flow channel ($C_0 = 2$, 1.779 and 1.675 for a circle, square and an equilateral triangle, respectively). The physical meaning of the two shape factors, C_0 in the Kozeny–Carman equation and C_α as defined in Bear and Bachmat (1990), is the same and hence $C_\alpha = C_0$ will be adopted in the later sections. As a special case, Appendix A demonstrates the equality of C_0 and C_α for flow along straight stream tubes in orthogonal directions without rigorous mathematical derivation for simplicity. Comparison of Eqs. (8) and (9) results in a hypothetical tortuosity factor associated with the Kozeny–Carman equation

$$\tau_{\mathrm{KC}} = \sqrt{\frac{a}{T^*_{\alpha 0}}\frac{C_\alpha}{C_0}} = \sqrt{\frac{a}{T^*_{\alpha 0}}}. \tag{10}$$

2.3 Comments on $T^*_{\alpha 0}$ Derived by Bear and Bachmat (1990)

Bachmat and Bear (1986) and Bear and Bachmat (1990) claimed $T^*_{\alpha 0} = \phi^S_\alpha/\phi_\alpha \le 1/3$ (with the equality sign valid for straight stream tubes only), by assuming that flow takes place along tortuous stream tubes that connect opposite sides of a cubic REV with sides parallel to the Cartesian x, y, z -axes, as illustrated in Fig. 2a. For straight tubes parallel to the axes and uniformly distributed in three orthogonal directions, $\phi^S_\alpha/\phi_\alpha \approx 1/3$. The corresponding tortuosity tensor $T^*_{\alpha ij} = (1/3)\delta_{ij}$ yields $\tau_{\mathrm{KC}} = \sqrt{2}$ for $T^*_{\alpha 0} = 1/3$, according to Eq. (10). However, this conclusion is questionable as one expects $\tau_{\mathrm{KC}} = 1$ when the flow direction is parallel to any of the axes for this specific case.

The above inconsistency can be partially resolved when the effective porosity $\phi_{\mathrm{e}\alpha}$ corresponding to the effective pore volume is used. Referring to Fig. 2a, when the flow direction is parallel to the x-axis, flow only takes place in tubes parallel to the x-axis and the stream tubes parallel to the y- and z-directions are inactive, yielding the effective porosity $\phi_{\mathrm{e}\alpha} = \phi_\alpha/3$ with ϕ_α being the total porosity. By replacing ϕ_α in Eq. (5) with $\phi_{\mathrm{e}\alpha}$, one has $T^*_{\alpha 0} = \phi^S_\alpha/\phi_{\mathrm{e}\alpha} = 3\phi^S_\alpha/\phi_\alpha = 1$. The result is also applicable to flows in y- and z-directions, which implies $T^*_{\alpha ij} = \delta_{ij}$. More details about the derivation of $T^*_{\alpha ij}$ for this specific case can

be found in Appendix A. The tortuosity factor from Eq. (10) becomes $\tau_{KC} = \sqrt{2/3}$, which is still different from what is expected, i.e. $\tau_{KC} = 1$.

For a porous medium, in a manner similar to that describing volume porosity and areal porosity, a linear porosity can be defined along a representative elementary length as the ratio between the summed length of void segments and the total length (Bear 1972; Kovács 1981). For randomly distributed pores, the equality of the average linear porosity and the areal porosity as well as the average areal porosity and volumetric porosity were proven in the Cartesian coordinate system (Bear 1972; Kovács 1981). This implies $T^*_{\alpha 0} = 1$ and $\tau_{KC} = \sqrt{2/3}$ for isotropic granular materials according to Eqs. (5) and (10), which is inconsistent with experimental results as the tortuosity factor τ_{KC} in the Kozeny–Carman equation is always larger than or equal to unity. Moreover, for most granular materials, it is also known that τ_{KC} generally decreases when the porosity of the material is increased. Unfortunately, such features of granular soils are not reflected by Eq. (5). This issue will be resolved in the following section by using a different approach based on the probability density function describing the directional random distribution of pores to determine the tortuosity tensor.

3 Tortuosity Tensor and Directional Distribution of Voids

In this section, a porous medium is considered as a discrete granular material with a random distribution of pores that connect with each other, which implies the effective porosity is the same as the total porosity.

3.1 Linear Porosity

The anisotropic nature of granular materials is characterized using the spatial distribution of pore voids described by a probability density function (Pietruszczak and Krucinski 1989; Masad and Muhunthan 2000). Consider a test line of length $L = 2R$ in direction $\boldsymbol{\nu}$ and passing the centre of the unit sphere in Fig. 1b. Let $l(\boldsymbol{\nu}) = \Sigma l_i(\boldsymbol{\nu})$ be the total length of intersections of this test line with pores. The fraction of this test line occupied by pores is referred to the linear porosity $\phi(\boldsymbol{\nu}) = l(\boldsymbol{\nu})/L$ in the direction of $\boldsymbol{\nu}$. $\phi(\boldsymbol{\nu})$ reflects the directional variation of the pore space and can be expressed as

$$\phi(\boldsymbol{\nu}) = \phi_0(1 + \Omega_{ij}\nu_i\nu_j + \Omega_{ijkl}\nu_i\nu_j\nu_k\nu_l + \cdots) \tag{11}$$

in which ϕ_0 is the average volumetric porosity of the material, Ω_{ij} and Ω_{ijkl} are symmetric traceless tensors. When only the first two terms are used, the directional distribution of pore space is simplified as

$$\phi(\boldsymbol{\nu}) = \phi_0(\delta_{ij} + \Omega_{ij})\nu_i\nu_j \tag{12}$$

For this case, if the eigenvalues of Ω_{ij} are distinct, $\phi(\boldsymbol{\nu})$ can reflect smooth orthogonal anisotropy. The symmetry axes of the orthogonal anisotropy are coincident with the principle axes of Ω_{ij}. If two eigenvalues of Ω_{ij} are equal, then $\phi(\boldsymbol{\nu})$describes the transverse isotropy (Pietruszczak and Krucinski 1989). It should be noted, however, using Eq. (12) may undermine some topology features of pore space and its spatial distribution, as Ω_{ij} is only the 'first approximation' as the measure of deviation from isotropy. The higher-rank traceless tensors Ω_{ijkl}, $\Omega_{ijkl\ldots}$ describe the higher order fluctuations and other features of void space distribution. Moreover, Ω_{ij} is unable to quantify the texture, roughness, size and shape of particles of granular materials.

3.2 Areal Porosity

Some inconsistency about the definition of areal porosity is found in the literature. When assuming that water flows through tortuous tubes (or flow channels), Bachmat and Bear (1986), Bear and Bachmat (1990) suggested that the areal porosity on the surface of a REV is no larger than 1/3, which results in $\phi_\alpha^S/\phi_\alpha \leq 1/3$ (or equivalently $\phi_\alpha^S/\phi_0 \leq 1/3$ when the material is fully saturated). This conclusion is different from the findings for materials with randomly distributed pores that the average linear porosity is the same as the areal porosity while the average areal porosity and volumetric porosity are identical in the Cartesian coordinate system (Bear 1972; Kovács 1981). This inconsistency is resolved by the following approach that takes into account the directional variation of pore voids.

Referring to Fig. 1b for a unit sphere enclosing a REV with anisotropic distribution of pore voids, at a point with the local out normal $\boldsymbol{\nu}$ on the surface of a unit sphere, the area occupied by voids (and hence the α-phase) within $\mathrm{d}S = \mathrm{d}x_1'\mathrm{d}x_2'$ with x_1' and x_2' defined in Fig. 1b can be expressed as

$$\mathrm{d}S_{\alpha\alpha} = \mathrm{d}x_1' \left(\phi(\boldsymbol{\nu}_2')\mathrm{d}x_2'\right) = \phi(\boldsymbol{\nu}_2')\mathrm{d}x_1'\mathrm{d}x_2'$$

or

$$\mathrm{d}S_{\alpha\alpha} = \left(\phi(\boldsymbol{\nu}_1')\mathrm{d}x_1'\right)\mathrm{d}x_2' = \phi(\boldsymbol{\nu}_1')\mathrm{d}x_1'\mathrm{d}x_2'$$

in which $\boldsymbol{\nu}_1' = (-\sin\varphi\ \cos\varphi\ 0)^T$ and $\boldsymbol{\nu}_2' = (\cos\theta\ \cos\varphi\ \cos\theta\ \sin\varphi\ -\sin\theta)^T$ define the directions of x_1' and x_2', respectively, $\mathrm{d}x_1' = R\sin\theta\mathrm{d}\varphi$, $\mathrm{d}x_2' = R\mathrm{d}\theta$. The average of the above two expressions is

$$\mathrm{d}S_{\alpha\alpha} = \frac{1}{2}\left[\phi(\boldsymbol{\nu}_1') + \phi(\boldsymbol{\nu}_2')\right]\mathrm{d}S = \phi_0\left[1 + \frac{1}{2}\Omega_{ij}\left(\nu_{1i}'\nu_{1j}' + \nu_{2i}'\nu_{2j}'\right)\right]\mathrm{d}S. \tag{13}$$

As $\boldsymbol{\nu}_1'$, $\boldsymbol{\nu}_2'$ and $\boldsymbol{\nu}$ are independent unit vectors orthogonal to each other, one has $\delta_{ij} = \nu_{1i}'\nu_{1j}' + \nu_{2i}'\nu_{2j}' + \nu_i\nu_j$. As such, Eq. (13) becomes

$$\mathrm{d}S_{\alpha\alpha} = \phi_0\left[1 + \frac{1}{2}\Omega_{ij}\left(\delta_{ij} - \nu_{\alpha i}\nu_{\alpha j}\right)\right]\mathrm{d}S = \phi_0\left(\delta_{ij} - \frac{1}{2}\Omega_{ij}\right)\nu_i\nu_j\mathrm{d}S \tag{14}$$

after applying $\Omega_{ii} = 0$. The directional variation of the local areal porosity on S_0 in the direction $\boldsymbol{\nu}$ is then expressed as

$$\phi_\alpha^S(\boldsymbol{\nu}) = \phi_0\left(\delta_{ij} - \frac{1}{2}\Omega_{ij}\right)\nu_i\nu_j \tag{15}$$

The total area occupied by voids on S_0 is determined as

$$S_{\alpha\alpha} = \phi_0\int_S\left[1 + \frac{1}{2}\Omega_{ij}\left(\delta_{ij} - \nu_i\nu_j\right)\right]\mathrm{d}S = 4\pi\phi_0$$

It follows the average areal porosity of the REV

$$\phi_\alpha^S = \frac{S_{\alpha\alpha}}{4\pi} = \phi_0 \tag{16}$$

which recovers the equality of the average linear porosity, the areal porosity and the volumetric porosity. For an anisotropic granular material, however, the linear porosity and the areal porosity in the direction of $\boldsymbol{\nu}$ are described by Eqs. (11) and (15), respectively.

3.3 Hydraulic Tortuosity

Consider an arbitrary test line with the length of $L = 2R$ in the direction of $\boldsymbol{\nu}$ and passing through the centre of the unit sphere shown in Fig. 1b. Given the linear porosity $\phi(\boldsymbol{\nu})$ in direction $\boldsymbol{\nu}$, the total length of interceptions of voids on the test line is $l(\boldsymbol{\nu}) = L\phi(\boldsymbol{\nu})$, which means that the probability for the void segments of this test line to intercept the sphere surface S_0 is $P_1 = l(\boldsymbol{\nu})/L = \phi(\boldsymbol{\nu})$. On the other hand, a solid test line intercepts the void fraction of S_0 with the probability of $P_2 = S_{\alpha\alpha}/(4\pi) = \phi_\alpha^S(\boldsymbol{\nu})$, with ϕ_α^S being the areal porosity of the REV. Consequently, the probability of the test line intercepts the voids at S_0 is

$$P(\boldsymbol{\nu}) = P_1 P_2 = \phi_\alpha^S(\boldsymbol{\nu})\phi(\boldsymbol{\nu}) \tag{17}$$

According to Eq. (3), the tortuosity tensor is calculated as

$$T^*_{\alpha ij} = \frac{1}{V_\alpha}\int_S P(\boldsymbol{\nu})\,\mathring{x}_i\,\nu_j \mathrm{d}S = \frac{1}{V_\alpha}\int_S \phi_\alpha^S(\boldsymbol{\nu})\phi(\boldsymbol{\nu})\,\mathring{x}_i\,\nu_j \mathrm{d}S \tag{18}$$

By applying Eq. (15), after some algebraic manipulations as given in the Appendix, one obtains

$$T^*_{\alpha ij} = \phi_0\left[\delta_{ij}\left(1 + \frac{1}{35}\Omega_{kl}\Omega_{kl}\right) + \frac{3}{7}\Omega_{ij} + \frac{4}{35}\Omega_{ik}\Omega_{kj}\right] \tag{19}$$

When neglecting the directional variation of $\phi_\alpha^S(\boldsymbol{\nu})$ by assuming a uniform random distribution of voids on S_0 with $\phi_\alpha^S(\boldsymbol{\nu}) = \phi_\alpha^S$, the tortuosity tensor is simplified to

$$T^*_{\alpha ij} = \frac{1}{V_\alpha}\frac{S_{\alpha\alpha}}{4\pi}\int_S R\phi_0(\delta_{kl} + \Omega_{kl})\nu_k\nu_l\nu_i\nu_j \mathrm{d}S = \phi_\alpha^S\left(\delta_{ij} + \frac{2}{5}\Omega_{ij}\right) \tag{20}$$

When neglecting the higher order terms of Ω_{ij}, the difference between the two expressions of $T^*_{\alpha ij}$ in Eqs. (19) and (20) is small, and hence Eq. (20) can be used for simplicity. For isotropic materials, both Eqs. (19) and (20) yield

$$T^*_{\alpha ij} = T^*_{\alpha 0}\delta_{ij}, \quad T^*_{\alpha 0} = \phi_\alpha^S \tag{21}$$

Different from the tortuosity tensor in Eq. (5), Eq. (21) shows that, for isotropic materials with random distribution of pores, $T^*_{\alpha 0}$ is the same as the average areal porosity ϕ_α^S on the surface of a spherical REV. Recall Eq. (16), the tortuosity of an isotropic granular material varies with the average porosity ϕ_0.

On the other hand, according to Dullien (1979), Bear (1972) and Bear and Bachmat (1990), $T^*_{\alpha 0}$ can be alternatively interpreted as the tortuosity of flow channels in a porous medium. As shown in the derivation of Bear and Bachmat (1990), the intrinsic phase average of a partial derivative of a quantity $\langle\nabla G\rangle_\mathrm{f}$ can be expressed as the gradient of the intrinsic phase average $\nabla\langle G\rangle_\mathrm{f}$ multiplied by $T^*_{\alpha ij}$ plus a surface integral over $S_{\alpha\beta}$. When neglecting absorption of the fluid phase on $S_{\alpha\beta}$ and diffusion into the solid phase, one has $\langle\nabla G\rangle_\mathrm{f} = \nabla\langle G\rangle_\mathrm{f}\cdot\mathbf{T}^*_\alpha$. In other words, $\mathbf{T}^*_\alpha$ reflects the geometrical characteristics of the microscopic domain occupied by the fluid. As such, for an isotropic medium, the tortuosity factor can be expressed as $\tau = (T^*_{\alpha 0})^{-1/2}$ by definition. Therefore, Eq. (21) leads to another expression for the tortuosity factor:

$$\tau = \left(\phi_\alpha^S\right)^{-1/2} \quad \text{or} \quad \tau = (\phi_0)^{-1/2} \tag{22}$$

4 Anisotropic Permeability and Directional Distribution of Voids

Referring to Eqs. (6) and (7), when determining the anisotropic permeability, α_{ij} as defined in Eq. (2) must be identified in addition to the tortuosity tensor $T^*_{\alpha ij}$. Using a different approach from that in Bear and Bachmat (1990), this study relates α_{ij} to tensor Ω_{ij} that describes the directional distribution of voids through the tortuosity tensor $T^*_{\alpha ij}$.

Referring to Fig. 1a, one has

$$\int\limits_{S_{0\alpha}} \overset{\circ}{x}_i \, \nu_{\alpha j} \mathrm{d}S = \int\limits_{S_{\alpha\alpha}} \overset{\circ}{x}_i \, \nu_{\alpha j} \mathrm{d}S + \int\limits_{S_{\alpha\beta}} \overset{\circ}{x}_i \, \nu_{\alpha j} \mathrm{d}S \tag{23}$$

As $S_{0\alpha} = \mathrm{S}_{\alpha\alpha} + \mathrm{S}_{\alpha\beta}$ is a closed surface with no internal singularity, applying the Gauss theorem to the left-hand side of Eq. (23) yields (Bear and Bensabat 1989)

$$\frac{1}{V_0} \int\limits_{S_{\alpha\alpha}} \overset{\circ}{x}_i \, \nu_{\alpha j} \mathrm{d}S + \frac{1}{V_0} \int\limits_{S_{\alpha\beta}} \overset{\circ}{x}_i \, \nu_{\alpha j} \mathrm{d}S = \frac{V_{0\alpha}}{V_0} \delta_{ij} \tag{24}$$

It follows that

$$\frac{1}{V_{0\alpha}} \int\limits_{S_{\alpha\beta}} \overset{\circ}{x}_i \, \nu_{\alpha j} \mathrm{d}S = \delta_{ij} - \frac{1}{V_{0\alpha}} \int\limits_{S_{\alpha\alpha}} \overset{\circ}{x}_i \, \nu_{\alpha j} \mathrm{d}S = \delta_{ij} - T^*_{\alpha ij} \tag{25}$$

The left-hand side term of Eq. (25) is the total static moment of the oriented elementary surface comprising the $S_{\alpha\beta}$-surface, with respect to planes passing through the centroid of the REV, per unit volume of the α-phase within V_0. This term may be estimated by replacing the fluid volume enclosed by $S_{\alpha\beta}$ using an equivalent hypothetical spherical sphere of the radius $R_{\mathrm{eq}} = 3\Delta_\alpha$ with the hydraulic radius $\Delta_\alpha = V_\alpha / S_{\alpha\beta}$ defined previously:

$$\frac{1}{V_{0\alpha}} \int\limits_{S_{\alpha\beta}} \overset{\circ}{x}_i \, \nu_{\alpha j} \mathrm{d}S = \frac{1}{V_{0\alpha}} \int\limits_{S_{\alpha\beta}} R_{\mathrm{eq}} \nu_{\alpha i} \nu_{\alpha j} \mathrm{d}S = \frac{3\Delta_\alpha}{V_{0\alpha}} \int\limits_{S_{\alpha\beta}} \nu_{\alpha i} \nu_{\alpha j} \mathrm{d}S \tag{26}$$

Recall Eq. (2), the above relation becomes

$$\frac{1}{V_{0\alpha}} \int\limits_{S_{\alpha\beta}} \overset{\circ}{x}_i \, \nu_{\alpha j} \mathrm{d}S = \frac{3\Delta_\alpha}{V_{0\alpha}} S_{\alpha\beta} \left(\delta_{ij} - \alpha_{ij} \right) = 3 \left(\delta_{ij} - \alpha_{ij} \right) \tag{27}$$

Inserting Eq. (27) into (25) yields

$$3 \left(\delta_{ij} - \alpha_{ij} \right) = \delta_{ij} - T^*_{\alpha ij} \Rightarrow \alpha_{ij} = \frac{1}{3} \left(2\delta_{ij} + T^*_{\alpha ij} \right) \tag{28}$$

By applying Eq. (19), α_{ij} is related to Ω_{ij} through

$$\alpha_{ij} = \frac{1}{3} \left(2\delta_{ij} + T^*_{\alpha ij} \right) = b_1 \delta_{ij} + b_2 \Omega_{ij} + b_3 \Omega_{ik} \Omega_{kj} \tag{29}$$

with

$$b_1 = \frac{1}{3} \left[2 + \phi_0 \left(1 + \frac{1}{35} \Omega_{kl} \Omega_{kl} \right) \right], \quad b_2 = \frac{\phi_0}{7}, \quad b_3 = \frac{4\phi_0}{105}$$

The inverse of α_{ij} is determined as

$$\alpha^{-1}_{ij} = \frac{1}{I_{\alpha 3}} \left(\alpha_{ik} \alpha_{kj} - I_{\alpha 1} \alpha_{ij} + I_{\alpha 2} \delta_{ij} \right), \tag{30}$$

where $I_{\alpha i}$ ($i = 1, 2$ and 3) are the three invariants of α_{ij} expressed as

$$\begin{aligned} I_{\alpha 1} &= \alpha_1 + \alpha_2 + \alpha_3 = 3b_1 + b_3 I_{\Omega 2} \\ I_{\alpha 2} &= \alpha_1\alpha_2 + \alpha_2\alpha_3 + \alpha_1\alpha_3 = 3b_1^2 + \left(b_2^2 - 4b_1 b_3\right) I_{\Omega 2} + 2b_3 I_{\Omega 2}^2 - 3b_2 b_3 I_{\Omega 3} \\ I_{\alpha 3} &= \alpha_1\alpha_2\alpha_3 = b_1^3 + b_1 b_2^2 I_{\Omega 2} + b_2^3 I_{\Omega 3} + b_3^2 \left(b_1 I_{\Omega 2}^2 + b_2 I_{\Omega 2} I_{\Omega 3} + b_3 I_{\Omega 3}^2\right) \\ &\quad -b_1 b_3 \left(2b_1 I_{\Omega 2} + 3b_2 I_{\Omega 3}\right) \end{aligned}$$

The permeability tensor given in Eq. (7) is then rewritten as

$$k_{ij} = \frac{\phi_0^4}{C_\alpha (1-\phi_0)^2 (\Sigma_{\alpha\beta}^{\beta})^2} \left[\delta_{ip}\left(1 + \frac{1}{35}\Omega_{kl}\Omega_{kl}\right) + \frac{3}{7}\Omega_{ip} + \frac{4}{35}\Omega_{ik}\Omega_{kp}\right] \frac{\alpha_{pq}\alpha_{qj} - I_{\alpha 1}\alpha_{pj} + I_{\alpha 2}\delta_{pj}}{I_{\alpha 3}} \tag{31}$$

For an isotropic medium, according to Eqs. (28) and (21), the tensor α_{ij} collapses to

$$\alpha_{ij} = a\delta_{ij}, \quad a = \frac{1}{3}\left(2 + T_{\alpha 0}^*\right) \tag{32}$$

Different from a constant of a= 2/3 proposed by Bear and Bachmat (1990), the value of a in Eq. (32) varies with $T_{\alpha 0}^*$ and hence with the tortuosity factor τ subject to Eq. (22). After applying Eq. (32) subject to Eq. (21), the expressions of permeability in Eqs. (8) and (31) for isotropic media are rewritten as:

$$k = \frac{\phi_0^3}{C_\alpha (1-\phi_0)^2 (\Sigma_{\alpha\beta}^{\beta})^2} \frac{3T_{\alpha 0}^*}{2 + T_{\alpha 0}^*} = \frac{3\phi_0^3 \phi_\alpha^s}{C_\alpha (1-\phi_0)^2 \left(2 + \phi_\alpha^s\right) (\Sigma_{\alpha\beta}^{\beta})^2} \tag{33}$$

As $\phi_\alpha^S = \phi_0$ for isotropic media (or equivalently uniformly distributed pore voids), an analogy of Eq. (33) with (9) yields a hypothetical tortuosity factor, expressed in Eq. (10), as

$$\tau_{\mathrm{KC}} = \sqrt{\frac{2 + T_{\alpha 0}^*}{3T_{\alpha 0}^*}} \tag{34}$$

Recall Eq. (21) and the fact $\phi_\alpha^S = \phi_0$, τ_{KC} is related to the mean porosity via

$$\tau_{\mathrm{KC}} = \sqrt{\frac{2 + \phi_0}{3\phi_0}} \tag{35}$$

which is very close to

$$\tau_{\mathrm{KC}} = (\phi_0)^{-0.4} \tag{36}$$

It is interesting to note that Eqs. (22) and (34) [or equivalently Eq. (36)] define the range of the tortuosity factor of granular materials with all connected, uniformly distributed pore voids in the form of $\tau = \phi_0^{-p}$. The value of p varies between 0.4 or 0.5, depending on how the tortuosity factor is determined.

For the special case discussed when flow takes place along stream tubes that connect opposite sides of a cubic REV with sides parallel to the Cartesian x, y, z-axes, the inconsistency as discussed in Sect. 2.3 is resolved by Eq. (34) together with the effective porosity concept, which results in $T_{\alpha ij}^* = \delta_{ij}$ (or $T_{\alpha 0}^* = 1$) and $\tau_{\mathrm{KC}} = 1$ according to Eq. (34).

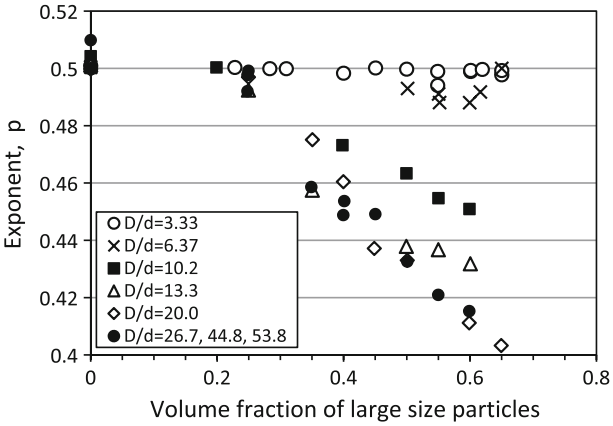

Fig. 3 Variation of p in $\tau(\phi) = \phi^{-p}$ with particle size and volume fraction in binary packing of spheres (Dias et al. 2006)

5 Comparison with Data in the Literature

5.1 Tortuosity and Permeability of Granular Materials as Functions of Porosity

When neglecting the effect of potential anisotropy, the relation $\tau_{KC} = \phi_0^{-p}$ with p in the range of 0.4–0.5 have been proven by both numerical modelling results and experimental data for different materials, including sand and mixtures of spherical particles, in the literature (e.g., Dullien 1979; Ho and Strieder 1981; Mauret and Renaud 1997; Mota et al. 2001; Dias et al. 2006 among others). In the numerous published data, it is worthwhile to examine the experimental results of Dias et al. (2006). The tortuosity factor in Dias et al. (2006) is τ_{KC} back-calculated from experimental permeability test results using the Kozeny–Carman equation by assuming the shape factor $C_0 = 2$ for the packing of spheres. The materials used were binary particulates of different particle diameter ratios D/d and varying volume fractions of large particles. They observed that for mono-size particulate bed and small particle diameter ratios, the value of p is always 0.5. With the increase of particle diameter ratio D/d (up to 53.8) and the volume fraction of large size particles (up to 0.65), the value of p gradually approaches 0.4, as shown in Fig. 3. As the randomness of the spheres packing increases as the particle diameter ratio and the volume fraction of large size particles are increased, one may conclude that the experimental results of Dias et al. (2006) are generally in agreement with Eq. (36) for random, uniform packing of spheres.

Equation (33) can be verified by examining the permeability–porosity relationship. Referring to Eqs. (9) and (33), the permeability can be expressed as

$$k_{KC} = \frac{f(\phi_0, \tau_{KC})}{C_0(\Sigma_{\alpha\beta}^{\beta})^2}; \quad f(\phi_0, \tau_{KC}) = \frac{\phi_0^3}{(1-\phi_0)^2\tau_{KC}^2} \tag{37}$$

in which τ_{KC} is given in Eq. (34) for the current work and $\tau_{KC} = \sqrt{2}$ in the Kozeny–Carman equation. Figure 4 presents the plot of the experimental hydraulic conductivity of Madison sand of $\phi_0 = 0.37 - 0.44$ (Das 2008) against $f(\phi_0, \tau_{KC})$ for the Kozeny–Carman equation and $f(\phi_0) = 3\phi_0^4/[(1-\phi_0)^2(2+\phi_0)]$ for Eq. (33). From this plot, it appears that both relations are equally good. Figure 5 shows the variation of the normalized permeability $k(1-\phi_0)^2$ in

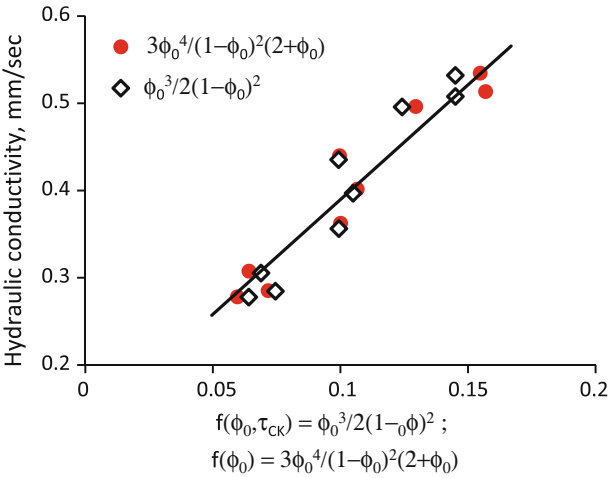

Fig. 4 Plot of hydraulic conductivity against porosity functions for Madison sand

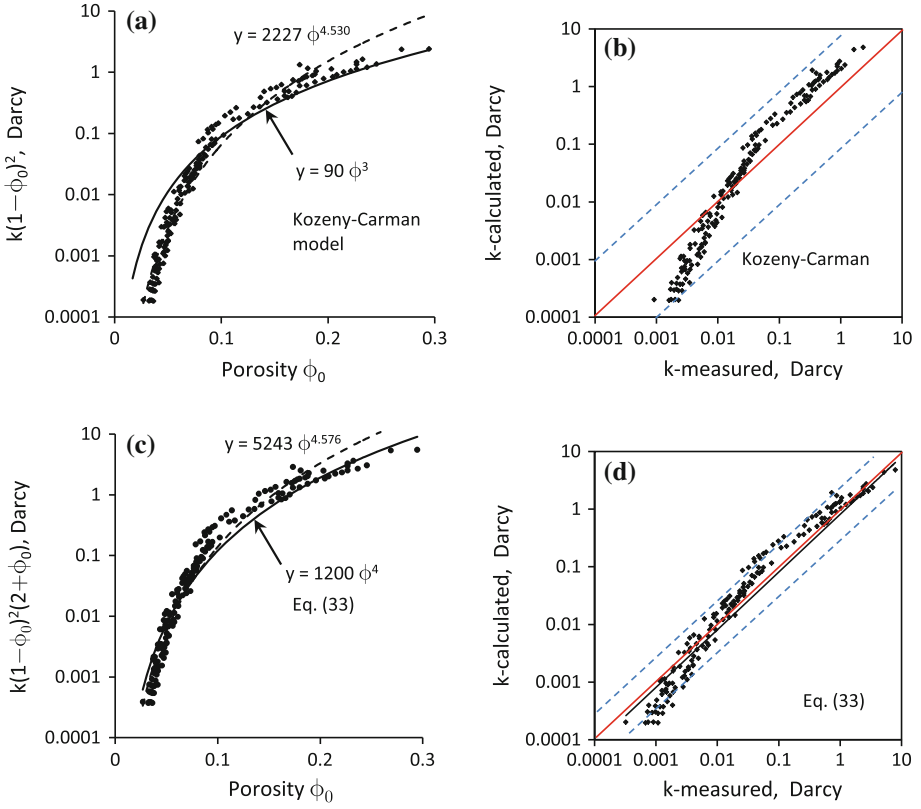

Fig. 5 Plot of normalized permeability against porosity for Fontainebleau Sandstone (data after Bourbié et al. 1987)

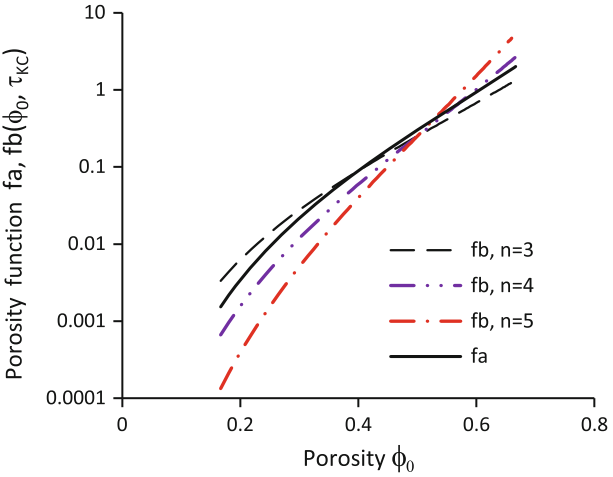

Fig. 6 Comparison of the porosity functions $f_a(\phi_0, \tau_{\mathrm{KC}})$ and $f_b(\phi_0, \tau_{\mathrm{KC}})$

Fig. 5a and $k(1-\phi_0)^2(2+\phi_0)$ in Fig. 5c against the porosity based on the measured data of Fontainebleau Sandstone (Bourbié et al. 1987; Gomez et al. 2010). The best fits according the least-square method are $k(1-\phi_0)^2 = 2{,}227\phi_0^{4.530}$ and $k(1-\phi_0)^2(2+\phi_0) = 5{,}243\phi_0^{4.576}$, respectively. The relation $k(1-\phi_0)^2(2+\phi_0) = 1{,}200\phi_0^4$ following Eq. (33) is also an equally good result, which is further demonstrated in Fig. 5d that compares the estimated k values using Eq. (33) with the measured data. However, the Kozeny–Carman equation fails to reproduce the measured data by almost one order, as can be observed from Fig. 5b.

Samarasinghe et al. (1982) suggested a slightly modified version of the Kozeny–Carman equation for normally consolidated clays as follows:

$$k = C\frac{e^n}{1+e} = C\frac{\phi_0^n}{(1-\phi_0)^{n-1}} \tag{38}$$

where C is a reference permeability that characterizes the materials, e the void ratio that is related to the porosity via $e = \phi_0/(1-\phi_0)$ and n an exponent generally in the range of 4–5. When $n = 3$, the Kozeny–Carman equation is recovered from Eq. (38). Similar to Eq. (37), let us introduce

$$f_a(\phi_0, \tau_{\mathrm{KC}}) = \frac{3\phi_0^3\phi_\alpha^S}{(1-\phi_0)^2\left(2+\phi_\alpha^S\right)} = \frac{3\phi_0^4}{(1-\phi_0)^2(2+\phi_0)} \quad \text{for Eq. (33)}$$

$$f_b(\phi_0, \tau_{\mathrm{KC}}) = \frac{\phi_0^n}{(1-\phi_0)^{n-1}\tau_{\mathrm{KC}}^2} \quad \text{for Eq. (37)}$$

As shown in Fig. 6, depending on the values of ϕ_0, the $f_a(\phi_0, \tau_{\mathrm{KC}})$ function is equivalent to $f_b(\phi_0, \tau_{\mathrm{KC}})$ with different n values. Table 1 summaries the range of n when $f_a(\phi_0, \tau_{\mathrm{KC}})$ is practically replicable with $f_b(\phi_0, \tau_{\mathrm{KC}})$ at different porosities. According to Table 1, one may expect that Eq. (33) is able to describe the permeability of clay at relatively high porosities. In addition, Fig. 6 and the data in Table 1 confirm that the modified Kozeny–Carman equation in Eq. (38) with $n = 3$ yields the same results as Eq. (33) for Madison sand of $\phi_0 = 0.37$–0.44, as shown in Fig. 4.

Table 1 The range of n when Eq. (38) is close to Eq. (33)

Porosity	Value of n
$\phi_0 < 0.4$	$n = 3$–4 but close to 3
$\phi_0 = 0.4$–0.5	$n \simeq 3$
$\phi_0 = 0.5$–0.53	$n \simeq 5$ but not sensitive to the value of n if it varies between 4 and 6
$\phi_0 = 0.53$–0.57	$n = 4$–5 but close to 4
$\phi_0 > 0.57$	$n = 3$–4 but close to 4

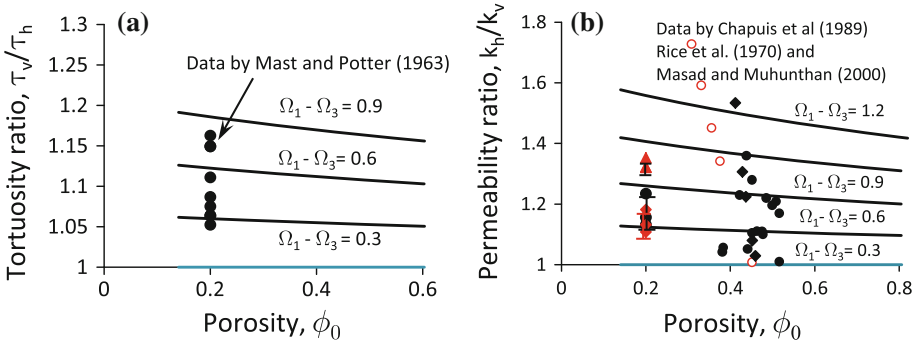

Fig. 7 **a** Theoretical and measured anisotropic tortuosity ratio $\tau_\perp/\tau_\parallel$, experimental data after Mast and Potter (1963); **b** theoretical and measured anisotropic permeability ratio $k_\parallel/k_\perp$, experimental data after Chapuis et al. (1989a); Rice et al. (1970) and Masad and Muhunthan (2000)

5.2 Tortuosity and Permeability of Anisotropic Granular Materials

This section provides a parametric study for cross-anisotropic media by assuming different directional pore space distributions quantified by the principal values of traceless tensor Ω_{ij}. Only cross-anisotropic granular materials are discussed, with the symbols $[\cdot]_\perp$ and $[\cdot]_\parallel$ being used to denote a quantity $[\cdot]$ when flow takes place in the direction of perpendicular to and parallel to the bedding plane, respectively. Herein, a bedding plane is referred to as the plane perpendicular to the deposition direction of solid particles during the preparation of soil specimens in laboratory tests or the formation of natural soils. The principal values of Ω_{ij} in the bedding plane are the major and intermediate ones with $\Omega_1 = \Omega_2$, while Ω_3 in the direction normal to the bedding plane satisfies $\Omega_3 = -2\Omega_1$. As limited experimental data are available in the literature for the tortuosity factors for flow along different directions in cross-anisotropic granular materials, only quantitatively comparison are made between the analytical results and the measured anisotropic tortuosity or the anisotropic permeability.

Figure 7 presents the variation of tortuosity factors $\tau_\perp$ and $\tau_\parallel$ with the average porosity ϕ_0 at different degrees of anisotropy quantified by $\Omega_1 - \Omega_3$. With the increase of $\Omega_1 - \Omega_3$, the anisotropic tortuosity ratio $\tau_\perp/\tau_\parallel$ ratio generally increases. For example, for materials of minor anisotropy with $\Omega_1 - \Omega_3 = 0.3$, $\tau_\perp/\tau_\parallel \approx 1.05 \pm 0.01$; when $\Omega_1 - \Omega_3 = 0.9$, the $\tau_\perp/\tau_\parallel$ ratio in the range of 1.13–1.19 at different ϕ_0 values, as shown in Fig. 7a. The permeability for flow parallel to the bedding plane, calculated from Eq. (31), is higher than that in the direction perpendicular to the bedding plane, with $k_\parallel/k_\perp = 1.10 \pm 0.02$ for $\Omega_1 - \Omega_3 = 0.3$ and 1.29–1.42 for $\Omega_1 - \Omega_3 = 0.9$, respectively (as shown in Fig. 7b).

The analytical results shown in Fig. 7 are qualitatively in agreement with experimental observations in the literature. Mast and Potter (1963) investigated the anisotropy of tortuosity of sand (with the average porosity $\phi_0 = 0.2$) through electrical resistance measurement. They observed higher tortuosity in the direction perpendicular to the bedding plane than that in the direction parallel to the bedding plane, with the ratio $\tau_\perp/\tau_\parallel = 1.05$–$1.16$ and the average of 1.11, as shown in Fig. 7a. Figure 7b shows that the $k_\parallel/k_\perp$ ratios, calculated from Eq. (31) at different values of ϕ_0 and $\Omega_1 - \Omega_3$, are in the same ranges of experimental results for different types of soils, as reported by Chapuis et al. (1989a), Rice et al. (1970) and Masad and Muhunthan (2000). It should be noted that no directional pore space distribution data is available for materials corresponding to the experimental $\tau_\perp/\tau_\parallel$ and $k_\parallel/k_\perp$ data in Fig. 7. Consequently, further investigation is necessary to verify Eq. (31) by measuring both Ω_{ij} and k_{ij} appropriately.

6 Concluding Remarks

This article presents a mathematical framework to determine the directional dependency of tortuosity and anisotropic permeability of porous media, using a structural measure describing the anisotropic distribution of pore voids. The key to successful implementation of this approach is the determination of directional variation of pores in porous media, which can be done through digital image analysis using different methods. The tortuosity tensor is derived based on a volume averaging approach and is related to the directional pore voids distribution. The permeability tensor is obtained from the macroscopic momentum balance equations of the fluid, which is related to the tortuosity tensor and eventually expressed as a function of the directional distribution of pore voids. When simplified to isotropic porous media, the theoretical analysis yields an explicit expression for the tortuosity as a function of porosity, which is in agreement with experimental data in the literature. The analytical results for anisotropic porous materials are qualitatively consistent with experimental observations, for both the measured tortuosity and the permeability of different materials. It is evident that the proposed approach is adequate in terms of describing the response of porous media exhibiting an inherent anisotropy. A systematic experimental study is ongoing for the verification of the proposed approach.

Acknowledgments Partial funding provided by the Natural Sciences and Engineering Research Council of Canada is gratefully acknowledged.

Appendix A: Determination of $T^*_{\alpha ij}$ for Flow Along Straight Stream Tubes in Orthogonal Directions

Let us re-examine the case when flow occurs along straight stream tubes that connect opposite sides of a cubic. It is assumed that the numbers of flow tubes are the same in all three directions, corresponding to the areal porosity of ϕ^s_α. For simplicity, we assume that there are N equal diameter tubes parallel to each axis. As such, the total intersection area of the tubes with each side is $S_{\alpha\alpha} = \phi^s_\alpha L^2$ and the total volume of the tubes is $V_\alpha = 3\phi^s_\alpha L^3$, which corresponds to $\phi_0 = 3\phi^s_\alpha$. If flow takes place parallel to an axis, only the flow tubes in this specific direction is active, which corresponds to an effective pore volume of $V_{e\alpha} = \phi^s_\alpha L^3$ and an effective porosity of $\phi_{e\alpha} = \phi^s_\alpha$. The probability for any test line starting from the centre of the REV and intersect the end of a stream tube on any side of the REV is $P_2(\nu) = \phi^s_\alpha$.

Replacing V_α with $V_{e\alpha}$ in Eq. (18), the tortuosity tensor is determined as

$$T^*_{\alpha ij} = \frac{1}{V_{e\alpha}} \int\limits_S \phi^s_\alpha \frac{L}{2} v_i v_j \mathrm{d}S = \frac{\phi^s_\alpha}{V_{e\alpha}} \int\limits_S \frac{L}{2} v_i v_j \mathrm{d}S = \frac{L}{2} \frac{\phi^s_\alpha}{V_{e\alpha}} (2L^2 \delta_{ij}) = \delta_{ij}$$

which yields $\alpha_{ij} = \delta_{ij}$, $T^*_{\alpha 0} = 1$. According to Eq. (7), the permeability corresponding to for flow along straight stream tubes is given as

$$k = \frac{\phi^3_\alpha}{C_\alpha (1-\phi_\alpha)^2 (\Sigma^\beta_{\alpha\beta})^2}$$

A comparison of the above relation with the Kozeny–Carman equation at $\tau = 1$ leads to $C_\alpha = C_0$.

Appendix B: Determination of $T^*_{\alpha ij}$ in Eq. (19)

By applying Eq. (15), $T^*_{\alpha ij}$ as expressed in Eq. (18) is determined as follows:

$$\begin{aligned}
T^*_{\alpha ij} &= \frac{1}{V_\alpha} \int\limits_S \phi_0 \left(\delta_{pq} - \frac{1}{2}\Omega_{pq}\right) v_p v_q R\phi_0 (\delta_{kl} + \Omega_{kl}) v_k v_l v_i v_j \mathrm{d}S \\
&= \frac{R\phi_0^2}{V_\alpha} \int\limits_S (\delta_{kl} + \Omega_{kl}) \left(\delta_{pq} - \frac{1}{2}\Omega_{pq}\right) v_p v_q v_k v_l v_i v_j \mathrm{d}S \\
&= \frac{4\pi R\phi_0^2}{3V_\alpha} \frac{3}{4\pi} \int\limits_S (\delta_{kl} + \Omega_{kl}) \left(\delta_{pq} - \frac{1}{2}\Omega_{pq}\right) v_p v_q v_k v_l v_i v_j \mathrm{d}S \\
&= \phi_0^{\frac{3}{4\pi}} \int\limits_S (\delta_{kl} + \Omega_{kl}) \left(\delta_{pq} - \frac{1}{2}\Omega_{pq}\right) v_p v_q v_k v_l v_i v_j \mathrm{d}S \\
&= \frac{3\phi_0}{4\pi} M_{ijklpq} (\delta_{kl} + \Omega_{kl}) \left(\delta_{pq} - \frac{1}{2}\Omega_{pq}\right) \\
&= \phi_0 \left(\delta_{ij} (1 + \frac{1}{35}\Omega_{kl}\Omega_{kl}) + \frac{3}{7}\Omega_{ij} + \frac{4}{35}\Omega_{ik}\Omega_{kj}\right)
\end{aligned}$$

where

$$\begin{aligned}
M_{ijklpq} &= \int\limits_S v_i v_j v_k v_l v_p v_q \mathrm{d}S \\
&= \frac{4\pi}{105} \left[\delta_{ij} \left(\delta_{kl}\delta_{pq} + \delta_{kp}\delta_{lq} + \delta_{kq}\delta_{lp}\right) + \delta_{ik} \left(\delta_{jl}\delta_{pq} + \delta_{jp}\delta_{lq} + \delta_{jq}\delta_{lp}\right)\right. \\
&\quad + \delta_{il} \left(\delta_{jk}\delta_{pq} + \delta_{jp}\delta_{kq} + \delta_{jq}\delta_{kp}\right) + \delta_{ip} \left(\delta_{jk}\delta_{lq} + \delta_{jl}\delta_{kq} + \delta_{jq}\delta_{kl}\right) \\
&\quad \left. + \delta_{iq} \left(\delta_{jk}\delta_{lp} + \delta_{jl}\delta_{kp} + \delta_{jp}\delta_{lk}\right)\right]
\end{aligned}$$

References

Al-Omari, A., Masad, E.: Three dimensional simulation of fluid flow in X-ray CT images of porous media. Int. J. Numer. Anal. Methods Geomech. **28**, 1327–1360 (2004). doi:10.1002/nag.389

Bachmat, Y., Bear, J.: Microscopic modelling of transport phenomena in porous media. I: the continuum approach. Transp. Porous Media **1**, 213–240 (1986)

Barrande, M., Bouchet, R., Denoyel, R.: Tortuosity of porous particles. Anal. Chem. **79**, 9115–9121 (2007)

Bear, J.: Dynamics of Fluids in Porous Media. Elsevier, New York (1972)

Bear, J., Bensabat, J.: Advective fluxes in multiphase porous media under nonisothermal conditions. Transp. Porous Media **4**(5), 423–448 (1989)

Bear, J., Bachmat, Y.: Introduction to Modeling of Transport Phenomena in Porous Media. Kluwer Academic Publishers, Dordrecht (1990)

Boudreau, B.P., Meysman, F.J.R.: Predicted tortuosity of muds. Geology **34**, 693–696 (2006)

Bourbié, T., Coussy, O., Zinszner, B.: Acoustics of Porous Media. Gulf Publishing Co., Houston (1987)

Carman, P.C.: Fluid flow through granular beds. Trans. Inst. Chem. Eng. **15**, 150–166 (1937)

Chapuis, R.P., Gill, D.E.: Hydraulic anisotropy of homogeneous soils and rocks: influence of the densification process. Bull. Eng. Geol. Environ. **39**(1), 75–86 (1989)

Chapuis, R.P., Gill, D.E., Baass, K.: Laboratory permeability tests on sand: influence of the compaction method on anisotropy. Can. Geotech. J. **26**, 614–622 (1989)

Clennell, M.B.: Tortuosity: a guide through the maze. In: Lovell, M.A., Harvey, P.K (eds.) Developments in Petrophysics, vol. 122, pp. 299–344. Geological Society, London. Special Publication (1997)

Comiti, J., Renaud, M.: A new model for determining mean structure parameters of fixed beds from pressure drop measurements: application to beds packed with parallelepipedal particles. Chem. Eng. Sci. **44**(7), 1539–1545 (1989)

Dagan, G.: Flow and Transport in Porous Formations. Springer, Heidelberg (1989)

Daigle, H., Dugan, B.: Permeability anisotropy and fabric development: a mechanistic explanation. Water Resour. Res. **47**(W12517), 1–11 (2011)

Das, B.M.: Advanced Soil Mechanics, 3rd edn. pp. 567 Taylor & Francis, London (2008)

Dias, R., Teixeira, J.A., Mota, M., Yelshin, A.: Tortuosity variation in a low density binary particulate bed. Sep. Purif. Technol. **51**(2), 180–184 (2006)

Diedericks, G.P.J., Du Plessis, J.P.: On tortuosity and areosity tensors for porous media. Transp. Porous Media **20**, 265–279 (1995)

Duda, A., Koza, Z., Matyka, M.: Hydraulic tortuosity in arbitrary porous media flow. Phys. Rev. E **84**, 036319 (2011)

Dullien, F.A.L.: Prediction of "tortuosity factors" from pore structure data. AIChE J. **21**, 820–822 (1975)

Dullien, F.A.L.: Porous Media: Fluid Transport And Pore Structure. Academic Press, New York (1979)

Gao, Y., Zhang, X., Rama, P., Liu, Y., Chen, R., Ostadi, H., Jiang, K.: Calculating the anisotropic permeability of porous media using the Lattice Boltzmann method and X-ray computed tomography. Transp. Porous Media **92**(2), 457–462 (2012)

Gomez, C.T., Dvorkin, J., Vanorio, T.: Laboratory measurements of porosity, permeability, resistivity, and velocity on Fontainebleau sandstones. Geophysics **75**(6), E191–E204 (2010)

Gommes, C.J., Bons, A.-J., Blacher, S., Dunsmuir, J.H., Tsou, A.H.: Practical methods for measuring the tortuosity of porous materials from binary or gray-tone tomographic reconstructions. AIChE J. **55**(8), 2000–2012 (2009)

Greenkorn, R.A., Kessler, D.P.: Dispersion in heterogeneous non-uniform anisotropic porous media. In: Flow through Porous Media (6th state-of-the-art Symposium sponsored by Industrial and Engineering Chemistry), 159–178, R.J. Nunge, Chairman, American Chemical Society Publications, Washington, DC, USA (1970)

Ho, F.-G., Strieder, W.: A variational calculation of the effective surface diffusion coefficient and tortuosity. Chem. Eng. Sci. **36**, 253–258 (1981)

Iversen, N., Jorgensen, B.B.: Diffusion coefficients of sulphate and methane in marine sediments: influence of porosity. Geochim. Cosmochim. Acta **57**, 571–578 (1993)

Jankovich, I., Fiori, A., Dagan, G.: Effective conductivity of an isotropic heterogeneous medium of lognormal conductivity distribution. Multiscale Model. Simul. **1**(1), 40–56 (2003)

Khan, F., Enzmann, F., Kersten, M., Wiegmann, A., Steiner, K.: 3D simulation of the permeability tensor in a soil aggregate on basis of nanotomographic imaging and LBE solver. J. Soil Sediment **12**(1), 86–96 (2012)

Kim, J.-H., Ochoa, J.A., Whitaker, S.: Diffusion in anisotropic porous media. Transp. Porous Media **2**, 327–356 (1987)

Kovács, G.: Seepage Hydraulics (Developments in Water Science), pp. 730. Elsevier, Amsterdam (1981)

Koza, Z., Matyka, M., Khalili, A.: Finite-size anisotropy in statistically uniform porous media. Phys. Rev. E **79**, 066306 (2009)
Kozeny, J.: Uber Kapillore Leintung des Wossers im Boden, Stizungsber. Akad. Wiss. Wien **136**, 271–306 (1927)
Kreamer, D.K., Weeks, E.P., Thompson, G.M.: A field technique to measure the tortuosity and sorption-affected porosity for gaseous diffusion in the unsaturated zone with experimental results from near Barnborehole. South Carolina. Water Resour. Res. **24**, 331–341 (1988)
Lanfrey, P.-Y., Kuzeljevic, Z.V., Dudukovic, M.P.: Tortuosity model for fixed beds randomly packed with identical particles. Chem. Eng. Sci. **65**(5), 1891–1896 (2010)
Masad, E., Muhunthan, B.: Three-dimensional characterization and simulation of anisotropic soil fabric. J. Geotech. Geoenviron. Eng. **126**(3), 199–207 (2000)
Mast, R.F., Potter, P.E.: Sedimentary structures, sand shape fabrics, and permeability. II. J. Geol. **71**(5), 548–565 (1963)
Matyka, M., Khalili, A., Koza, Z.: Tortuosity–porosity relation in the porous media flow. Phys. Rev. E **78**, 026306 (2008)
Mauret, E., Renaud, M.: Transport phenomena in multi-particle systems-I. Limits of applicability of capillary model in high voidage beds–application to fixed beds of fibers and fluidized beds of spheres. Chem. Eng. Sci. **52**(11), 1807–1817 (1997)
Mota, M., Teixeira, J.A., Yelshin, A.: Binary spherical particle mixed beds porosity and permeability relationship measurement. Trans. Filtr. Soc. **1**, 101–106 (2001)
Ohkubo, T.: Tortuosity based on anisotropic diffusion process in structured plate-like obstacles by Monte Carlo simulation. Transp. Porous Media **72**, 339–350 (2008)
Pietruszczak, S., Krucinski, S.: Description of anisotropic response of clays using a tensorial measure of structural disorder. Mech. Mater. **8**, 237–249 (1989)
Rice, P.A., Fontugne, D.J., Latini, R.G., Barduhn, A.J.: Anisotropic permeability in porous media. Ind. Eng. Chem. **62**, 23–31 (1970)
Salem, H., Chilingarian, G.V.: Influence of porosity and direction of flow on tortuosity in unconsolidated porous media. Energy Source **22**, 207–213 (2000)
Samarasinghe, A.M., Huang, Y.M., Drnecich, V.P.: Permeability and consolidation of normally consolidated soils. J. Geotech. Eng. **108**(GT6), 835–850 (1982)
Scheidegger, A.E.: Directional permeability of porous media to homogeneous fluids. Geofis. Pura. Appl. **28**, 75–90 (1954)
Selomulya, C., Tran, T.M., Jia, X., Williams, R.A.: An integrated methodology to evaluate permeability from measured microstructures. AIChE J. **52**(10), 3394–3400 (2006)
Suribhatla, R., Jankovic, I., Fiori, A., Dagan, G.: Effective conductivity of an anisotropic heterogeneous medium of random conductivity distribution. Multiscale Model. Simul. **9**(3), 933–954 (2011)
Weissberg, H.: Effective diffusion coefficients in porous media. J. App. Phys. **34**, 2636–2639 (1963)
Whitaker, S.: Flow in porous media I: a theoretical derivation of Darcy's law. Transp. Porous Media **1**, 3–25 (1986)
Whitaker, S.: The Method of Volume Averaging. Kluwer Academic Publishers, Dordrecht (1999)
Witt, K.-J., Brauns, J.: Permeability-anisotropy due to particle shape. J. Geotech. Eng. **109**(9), 1181–1187 (1983)
Yazdchi, K., Srivastava, S., Luding, S.: Microstructural effects on the permeability of periodic fibrous porous media. Int. J. Multiphase Flow **37**(8), 956–966 (2011)